

Dear authors,

Thank you very much for your contribution to Chinese Physics B.

Your paper has been published in Chinese Physics B, 2014, Vol.23, No.8.

Attached is the PDF offprint of your published article, which will be convenient and helpful for your communication with peers and coworkers.

Readers can download your published article through our website


<http://www.iop.org/cpb> or <http://cpb.iphy.ac.cn>

What follows is a list of related articles published recently in Chinese Physics B.

---


#### Complete coverage of reduced graphene oxide on silicon dioxide substrates

Huang Jingfeng, Melanie Larisika, Chen Hu, Steve Faulkner, Myra A. Nimmo, Christoph Nowak, Alfred Tok ling Yoong

Chin. Phys. B , 2014, 23(8): 088103.Full Text:  [PDF](#) (516KB)


#### An optimized, sensitive and stable reduced graphene oxide-gold nanoparticle-luminol-H<sub>2</sub>O<sub>2</sub> chemiluminescence system and its potential analytical application

Wang Wen-Shuo, He Da-Wei, Wang Ji-Hong, Duan Jia-Hua, Peng Hong-Shang, Wu Hong-Peng, Fu Ming, Wang Yong-Sheng, Zhang Xi-Qing

Chin. Phys. B , 2014, 23(4): 048103.Full Text:  [PDF](#) (826KB)


#### Coupling interaction between a single emitter and the propagating surface plasmon polaritons in a graphene microribbon waveguide

Zhang Lei, Fu Xiu-Li, Lei Ming, Chen Jian-Jun, Yang Jun-Zhong, Peng Zhi-Jian, Tang Wei-Hua

Chin. Phys. B , 2014, 23(3): 038101.Full Text:  [PDF](#) (2420KB)


#### Transparent conductive graphene films prepared by hydroiodic acid and thermal reduction

Qin Meng-Meng, Ji Wei, Feng Yi-Yu, Feng Wei

Chin. Phys. B , 2014, 23(2): 028103.Full Text:  [PDF](#) (1681KB)


#### Controlled construction of nanostructures in graphene

Li Zhong-Jun, Li Qiang, Cheng Zeng-Guang, Li Hong-Bian, Fang Ying

Chin. Phys. B , 2014, 23(2): 028102.Full Text:  [PDF](#) (570KB)

#### Crystallization of polymer chains induced by graphene: Molecular dynamics study

Yang Jun-Sheng, Huang Duo-Hui, Cao Qi-Long, Li Qiang, Wang Li-Zhi, Wang Fan-Hou

Chin. Phys. B , 2013, 22(9): 098101.Full Text:  [PDF](#) (958KB)

---

---

中国物理 **B**  
**Chinese  
Physics B**

---

Volume 23 Number 8 August 2014

Formerly *Chinese Physics*

---

A Series Journal of the Chinese Physical Society  
Distributed by IOP Publishing

---

Online: [iopscience.iop.org/cpb](http://iopscience.iop.org/cpb)  
[cpb.iphy.ac.cn](http://cpb.iphy.ac.cn)

---

# Effects of graphene defects on Co cluster nucleation and intercalation\*

Xu Wen-Yan(徐文焱)<sup>a)b)</sup>, Huang Li(黄立)<sup>a)b)</sup>, Que Yan-De(阙炎德)<sup>a)b)</sup>, Lin Xiao(林晓)<sup>b)a)†</sup>, Wang Ye-Liang(王业亮)<sup>a)b)‡</sup>, Du Shi-Xuan(杜世萱)<sup>a)b)</sup>, and Gao Hong-Jun(高鸿钧)<sup>a)b)§</sup>

<sup>a)</sup>Institute of Physics, Chinese Academy of Sciences, Beijing 100190, China

<sup>b)</sup>University of Chinese Academy of Sciences, Beijing 100049, China

(Received 9 April 2014; revised manuscript received 4 May 2014; published online 10 June 2014)

Four kinds of defects are observed in graphene grown on Ru (0001) surfaces. After cobalt deposition at room temperature, the cobalt nanoclusters are preferentially located at the defect position. By annealing at 530 °C, cobalt atoms intercalate at the interface of Graphene/Ru (0001) through the defects. Further deposition and annealing increase the sizes of intercalated Co islands. This provides a method of controlling the arrangement of cobalt nanoclusters and also the density and the sizes of intercalated cobalt islands, which would find potential applications in catalysis industries, magnetism storage, and magnetism control in future information technology.

**Keywords:** graphene, defects, cobalt, intercalation, scanning tunneling microscopy

**PACS:** 81.05.ue, 87.64.Dz, 68.55.Ln, 68.55.at

**DOI:** 10.1088/1674-1056/23/8/088108

## 1. Introduction

Graphene, a single layer of carbon atoms densely packed by  $sp^2$  hybrid bonding, is a potential candidate for many applications due to its outstanding structural, electronic, mechanical, and thermal properties.<sup>[1–3]</sup> One of these applications is for it to be used as a thin film template to control the size and arrangement of metal nanoclusters.<sup>[4]</sup> Metal nanoclusters exhibit the quantum size effect<sup>[5]</sup> and unusual chemical reactivity,<sup>[6]</sup> which could be utilized widely in electronics and catalysis industries. In particular, cobalt nanoclusters exhibit strong magnetism.<sup>[7]</sup> The arrangement of Co clusters on a graphene template may be affected by the structural defects in graphene. Therefore, using graphene with defects as a template to control the size and arrangement of metal nanoclusters can produce new phenomena and offer a broad potential for useful applications.

## 2. Methods

Our experiments were carried out in a UHV system with a base pressure lower than  $2 \times 10^{-10}$  mbar (1 bar =  $10^5$  Pa). The system is equipped with an Omicron room temperature scanning tunneling microscope (RT-STM), an electron beam heater (EBH), a low energy electron diffraction (LEED), a UHV evaporator with a cobalt rod (purity of 99.995%, Alfa Aesar), and a gas station that can introduce ethylene (purity of 99.995%, Beijing Huayuan Gas Chemical Industry Co., Ltd) into the UHV chamber through a leak valve. Epitaxial growth

of graphene on metals<sup>[8–11]</sup> is a very important method to produce graphene. Single-crystal Ru (0001), purchased from MaTeck, was used as the substrate for the epitaxial growth of graphene. The Ru (0001) surfaces were prepared by repeated cycles of  $Ar^+$  sputtering and annealing in oxygen at 800 °C to remove the residual carbon, and then flashing to 1300 °C to remove the oxide.<sup>[12]</sup> The surface order and cleanliness were verified by LEED, Auger electron spectroscopy (AES), and STM. The graphene layer was prepared by thermal decomposition of ethylene on a Ru (0001) surface at a temperature of 800 °C.<sup>[12]</sup>

## 3. Results and discussion

It is well known that the graphene grown on Ru (0001) substrate forms a regular Moiré pattern; there are three different sites, i.e., atop, fcc, and hcp sites within the Moiré unit cell.<sup>[13]</sup> In our experiments, two kinds of point defect are found, i.e., adatoms and vacancies. As shown in Fig. 1(a), an contaminant adatom is located in the hcp region of the graphene/Ru (0001) Moiré structure. No interference is observed around this adatom defect in the atomic-resolved STM images, which concludes the intactness of the graphene structure. The other kind of point defect, i.e., vacancy, is shown in Fig. 1(b). Unlike the adatom, the loss of carbon atoms in the graphene structure leads to a complex interference around the defect position, which is different from the interference patterns in free-standing graphene, owing to strong interactions between the graphene and the Ru substrate.<sup>[14]</sup> Besides

\*Project supported by Funds from the Ministry of Science and Technology of China (Grant Nos. 2013CBA01600 and 2011CB932700), the National Natural Science Foundation of China (Grant Nos. 61222112 and 11334006), and the Funds from the Chinese Academy of Sciences.

†Corresponding author. E-mail: [xlin@ucas.ac.cn](mailto:xlin@ucas.ac.cn)

‡Corresponding author. E-mail: [ylwang@iphy.ac.cn](mailto:ylwang@iphy.ac.cn)

§Corresponding author. E-mail: [hjgao@iphy.ac.cn](mailto:hjgao@iphy.ac.cn)

point defects, two kinds of line defects are shown in Figs. 1(c) and 1(d). The most common line defects are graphene edges as shown in Fig. 1(c). In the upper-left and middle parts of the image, the graphene/Ru (0001) structure with Moiré pattern is shown, while other parts of the surface are covered by amorphous carbon. The surface step edge of the Ru crystal is another important source of the line defects. In most cases a graphene sheet grows in the ‘downhill’ direction and can flow uninhibitedly in a carpet-like fashion across the step.<sup>[15]</sup> However, we also find that steps might interrupt the expansion of graphene and induce line defects along step edges as shown in Fig. 1(d). One possible reason could be that there are two nucleation centers on the two terraces of the Ru (0001) surface from which two graphene sheets develop separately. In total, four kinds of defect are found, i.e., two point defects and two line defects.

After the growth of graphene on Ru surfaces, cobalt atoms are deposited from the cobalt evaporator onto the graphene Moiré template at room temperature. An STM image of graphene after cobalt deposition is shown in Fig. 2(a). The cobalt forms three-dimensional (3D) clusters whose bottom diameter and height are typically  $\sim 5$  nm and  $\sim 2$  nm respectively; each cluster contains hundreds of cobalt atoms (Figs. 2(b) and 2(c)), which is different from the monodispersed Pt nanocluster with a preferred nucleation region on the Moiré template of graphene/Ru (0001).<sup>[4]</sup> On defect-free graphene surfaces, cobalt clusters nucleate randomly on the surface at the coverage of 0.02 ML (Fig. 2(a)), while on the graphene with defects, cobalt cluster nucleation possesses different properties. A series of STM images with Co coverages of 0.02, 0.06, and 0.36 ML is shown in Figs. 2(d)–2(f). A large proportion of cobalt clusters are located near defects in

graphene as shown in Fig. 2(d). We infer that the cobalt atom preferential adsorptions in these regions are due to the bigger adsorption energies at these positions which come from dangling bonds of the carbon atoms or bare ruthenium surface at defects. At increasing coverages, a large proportion of cobalt clusters nucleate near point defects in graphene while few cobalt clusters are located at the line defects on steps as shown in Fig. 2(f). Therefore, defects in graphene whose density can be controlled by the sputtering of ions/electrons or growth conditions provide a method to modulate the arrangement of cobalt nanoclusters on graphene.

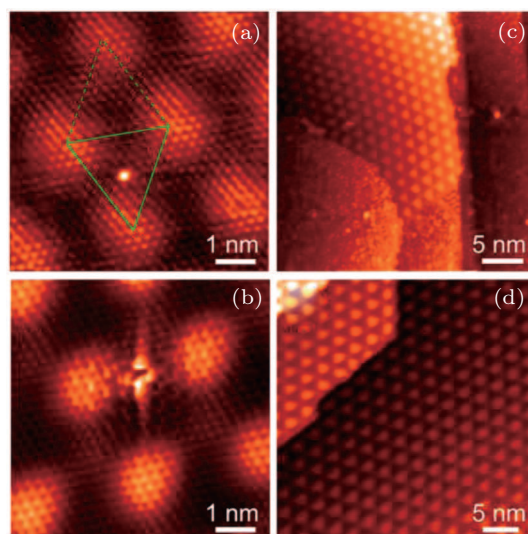


**Fig. 1.** (color online) STM images of different kinds of defects in graphene. (a) STM image of graphene with adatom. The Moiré unit cell is shown, in which the atop sites are the bright area, and hcp and fcc sites are marked by the solid and dotted lines, respectively. (b) STM image of graphene with vacancy. (c) STM image of graphene with edges next to the surface covered by amorphous carbon. (d) STM image of graphene with edge on the step edge of Ru substrate.

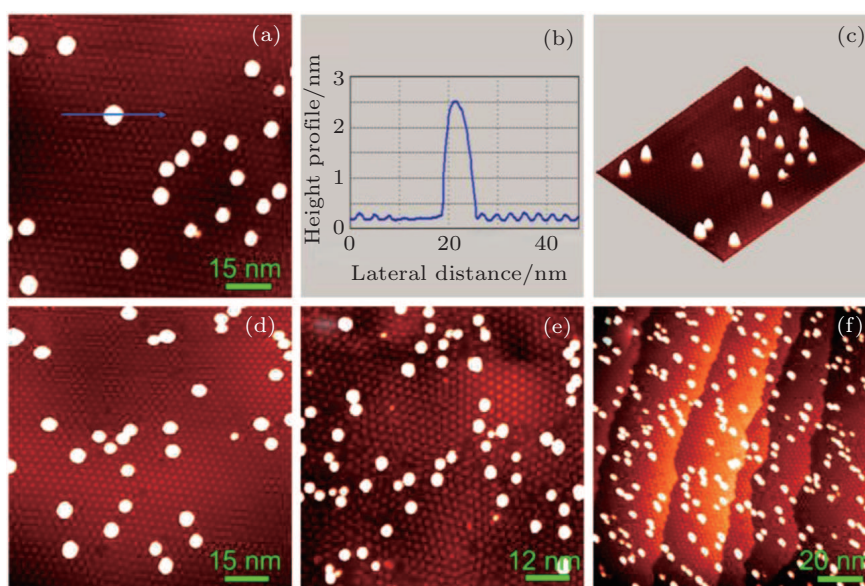


**Fig. 2.** (color online) STM images of graphene with cobalt clusters. (a) STM image of graphene without defects after cobalt deposition. (b) Line profile along the blue line shown in panel (a). (c) Corresponding 3D image of panel (a). (d)–(f) STM images of graphene with defects after cobalt deposition at 0.02 ML (d), 0.06 ML (e), and 0.36 ML (f).

There is a strong interaction between epitaxial graphene and the Ru substrate, which disturbs many unique electronic properties of graphene. Previous studies have reported that the interaction can be effectively weakened by the intercalation of other elements, such as noble metals Ag,<sup>[16,17]</sup> Pt,<sup>[18]</sup> Pd,<sup>[18]</sup> and Au,<sup>[18–21]</sup> magnetic metals Ni<sup>[18]</sup> and Co,<sup>[18]</sup> the IIIA group metal In,<sup>[18]</sup> the rare earth metal Ce,<sup>[18]</sup> and Cu,<sup>[22]</sup> between epitaxial graphene and the substrate. Here, we report the influence of defects in graphene on cobalt intercalation between epitaxial graphene and the Ru substrate. Cobalt atoms intercalate between graphene and Ru (0001) when annealing at 530 °C. After Co intercalation, graphene exhibits a similar Moiré pattern on the intercalated structures to that on Ru (0001), which is shown by STM images in Fig. 3(a). Most of the intercalated cobalt islands are under or near defects in graphene. It can be inferred that the defects in graphene afford a path for the intercalation process of cobalt atoms. We

deposit additional Co atoms onto the Co interacted graphene sample, find that the additional Co atoms form nanoclusters and the arrangement of cobalt nanoclusters is also affected by defects in graphene, as the topographic image demonstrates in Fig. 3(b). After subsequently annealing at 530 °C again, all the cobalt atoms on the graphene intercalate between graphene and Ru (0001), and the sizes of the intercalated cobalt islands increase. But the density of intercalated cobalt islands almost remains the same as that in the first cobalt intercalation cycle, which is because the density of defects in graphene does not change in the process. Accordingly we can control the density and size of intercalated cobalt islands by adjusting the density of the defects and the coverage of the Co atoms. Considering the magnetism of cobalt clusters and the protection from the inert graphene layer, this intercalated graphene/Co/Ru (0001) structure would be very useful in many fields.

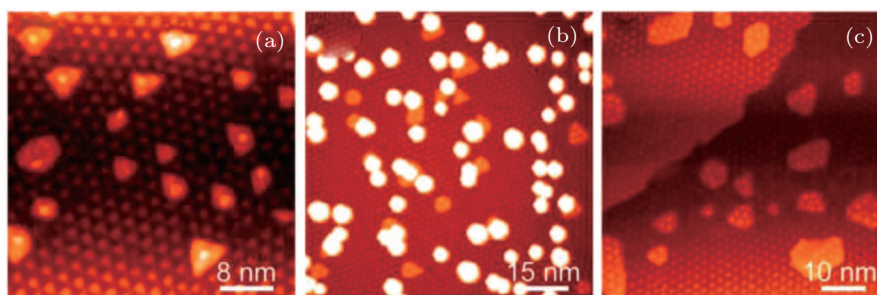


**Fig. 3.** (color online) STM images of graphene after cobalt intercalation. (a) STM image of graphene after cobalt deposition and annealing at 530 °C. The brighter parts of the image are cobalt islands under graphene. (b) STM image of graphene after cobalt intercalation and the additional cobalt deposition. (c) STM image of graphene after two cycles of cobalt intercalation.

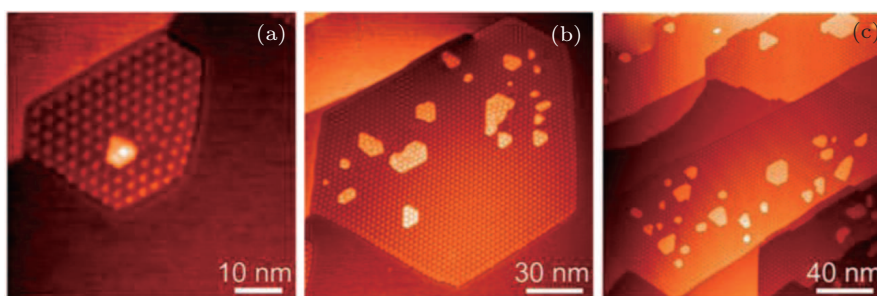


**Fig. 4.** (color online) STM images of graphene islands with different sizes after cobalt intercalation. (a) STM image of a graphene island with a lateral size of about 40 nm after cobalt intercalation. The brighter part of the graphene island is the cobalt island under the graphene. (b) STM image of a graphene island with a lateral size of about 150 nm after cobalt intercalation. (c) STM image of graphene islands with lateral sizes exceeding 250 nm after cobalt intercalation.

In addition to one full monolayer continuous graphene, cobalt intercalation on graphene islands is also explored. The method of growing graphene islands is temperature-programmed growth (TPG). The Ru (0001) substrate is exposed to 100-L ethylene at room temperature, followed by annealing at 830 °C. The sample is kept at that temperature for 30 s and then cooled down to room temperature at a rate

of 0.5 °C·s<sup>-1</sup>.<sup>[23]</sup> STM topographic images (Figs. 4(a)–4(c)) show the graphene islands after cobalt intercalation. Like the case of cobalt islands under full monolayer graphene, the intercalated cobalt islands also mostly located under or on the neighborhood of defects in the graphene islands. For different sizes of graphene islands there are only a few intercalated cobalt islands near the edge of graphene islands, which may be

attributed to the fact that most of cobalt atoms near the edge of graphene islands diffuse into bare Ru surface during annealing. These observations further demonstrate that the defects in graphene benefit the formation of a cobalt intercalated structure under graphene.

#### 4. Conclusions

We present four kinds of defects in graphene on Ru (0001). The deposited cobalt atoms prefer to be located near these defects and demonstrate a distribution of nanoclusters on graphene at room temperature. The arrangement and density of cobalt nanoclusters on graphene are modulated by controlling the density of defects in graphene. After the sample is annealed, cobalt atoms intercalate under graphene and form intercalated cobalt islands neighboring the defects. The additional deposition and intercalation cycles increase the sizes of intercalated cobalt islands without changing the density of cobalt islands. Therefore our work affords a method to modulate the density of cobalt nanoclusters and the arrangement of intercalated cobalt islands under graphene by artificially controlling the density of defects in graphene. This would be very useful in catalysis industries, magnetism storage, and magnetism control in future information technology.

#### References

- [1] Novoselov K S, Geim A K, Morozov S V, Jiang D, Zhang Y, Dubonos S V, Grigorieva I V and Firsov A A 2004 *Science* **306** 666  
 [2] Müllen K and Rabe J P 2008 *Acc. Chem. Res.* **41** 511

- [3] Park S and Ruoff R S 2009 *Nat. Nanotechnol.* **4** 217  
 [4] Pan Y, Gao M, Huang L, Liu F and Gao H J 2009 *Appl. Phys. Lett.* **95** 093106  
 [5] Halperin W P 1986 *Rev. Mod. Phys.* **58** 533  
 [6] Boyen H G, Kastle G, Weigl F, Koslowski B, Dietrich C, Ziemann P, Spatz J P, Riethmuller S, Hartmann C, Moller M, Schmid G, Garnier M G and Oelhafen P 2002 *Science* **297** 1533  
 [7] Billas I M L, Chatelain A and de Heer W A 1994 *Science* **265** 1682  
 [8] Pan Y, Shi D X and Gao H J 2007 *Chin. Phys.* **16** 3151  
 [9] Sutter P W, Flege J I and Sutter E A 2008 *Nat. Mater.* **7** 406  
 [10] Pan Y, Zhang H G, Shi D X, Sun J T, Du S X, Liu F and Gao H J 2009 *Adv. Mater.* **21** 2777  
 [11] Kim K S, Zhao Y, Jang H, Lee S Y, Kim J M, Kim K S, Ahn J H, Kim P, Choi J Y and Hong B H 2009 *Nature* **457** 706  
 [12] Mao J H, Huang L, Pan Y, Gao M, He J F, Zhou H T, Guo H M, Tian Y, Zou Q, Zhang L Z, Zhang H G, Wang Y L, Du S X, Zhou X J, Castro Neto A H and Gao H J 2012 *Appl. Phys. Lett.* **100** 093101  
 [13] Wintterlin J and Bocquet M L 2009 *Surf. Sci.* **603** 1841  
 [14] Rutter G M, Crain J N, Guisinger N P, Li T, First P N and Stroscio J A 2007 *Science* **317** 219  
 [15] Coraux J, N'Diaye A T, Busse C and Michely T 2008 *Nano Lett.* **8** 565  
 [16] Farías D, Shikin A M, Rieder K H and Dedkov Y S 1999 *J. Phys.: Condens. Matter* **11** 8453  
 [17] Starodubov A G, Medvetzki M A, Shikin A M and Adamchuk V K 2004 *Phys. Solid State* **46** 1340  
 [18] Huang L, Pan Y, Pan L D, Gao M, Xu W Y, Que Y D, Zhou H T, Wang Y L, Du S X and Gao H J 2011 *Appl. Phys. Lett.* **99** 163107  
 [19] Shikin A M, Prudnikova G V, Adamchuk V K, Moresco F and Rieder K H 2000 *Phys. Rev. B* **62** 13202  
 [20] Varykhalov A, Sánchez-Barriga J, Shikin A M, Biswas C, Vescovo E, Rybkin A, Marchenko D and Rader O 2008 *Phys. Rev. Lett.* **101** 157601  
 [21] Enderlein C, Kim Y S, Bostwick A, Rotenberg E and Horn K 2010 *New J. Phys.* **12** 033014  
 [22] Dedkov Y, Shikin A, Adamchuk V, Molodtsov S, Laubschat C, Bauer A and Kaindl G 2001 *Phys. Rev. B* **64** 035405  
 [23] Huang L, Xu W Y, Que Y D, Pan Y, Gao M, Pan L D, Guo H M, Wang Y L, Du S X and Gao H J 2012 *Chin. Phys. B* **21** 088102

JUST FOR AUTHORS  
 — CHINESE PHYSICS B

# Chinese Physics B

Volume 23

Number 8

August 2014

**088101 Introduction to *ChinaNANO* 2013**

Wei Zhi-Xiang and Zhu Xing

**INVITED REVIEW — International Conference on Nanoscience & Technology, China 2013**

**086801 Dye-sensitized solar cells: Atomic scale investigation of interface structure and dynamics**

Ma Wei, Zhang Fan and Meng Sheng

**087801 Three-dimensional noble-metal nanostructure: A new kind of substrate for sensitive, uniform, and reproducible surface-enhanced Raman scattering**

Tian Cui-Feng, You Hong-Jun and Fang Ji-Xiang

**088102 Silicon nanoparticles: Preparation, properties, and applications**

Chang Huan and Sun Shu-Qing

**088801 Functionalization of carbon nanotubes/graphene by polyoxometalates and their enhanced photo-electrical catalysis**

Zhang Shuang-Shuang, Liu Rong-Ji, Zhang Guang-Jin and Gu Zhan-Jun

**SPECIAL TOPIC — International Conference on Nanoscience & Technology, China 2013**

**083301 Electromagnetic wave absorbing properties and hyperfine interactions of Fe–Cu–Nb–Si–B nanocomposites**

Han Man-Gui, Guo Wei, Wu Yan-Hui, Liu Min and Magundappa L. Hadimani

**084201 High refractive index sensitivity sensing in gold nanoslit arrays**

Yuan Jun, Kan Qiang, Geng Zhao-Xin, Xie Yi-Yang, Wang Chun-Xia and Chen Hong-Da

**086101 Synthesis of boron, nitrogen co-doped porous carbon from asphaltene for high-performance supercapacitors**

Zhou Ying, Wang Dao-Long, Wang Chun-Lei, Jin Xin-Xin and Qiu Jie-Shan

**086102 Enhanced photoluminescence of CdSe quantum dots by the coupling of Ag nanocube and Ag film**

Jiang Tong-Tong, Shao Wei-Jia, Yin Nai-Qiang, Liu Ling, Song Jiang-Lu-Qi, Zhu Li-Xin and Xu Xiao-Liang

**086201 Microwave ferromagnetic properties of as-deposited Co<sub>2</sub>FeSi Heusler alloy films prepared by oblique sputtering**

Cao Xiao-Qin, Li Shan-Dong, Cai Zhi-Yi, Du Hong-Lei, Xue Qian, Gao Xiao-Yang and Xie Shi-Ming

**086802 Adsorptions and diffusions of carbon atoms on the surface and in the subsurface of Co (200): a first-principles density-functional study**

Qiao Liang, Wang Shu-Min, Zhang Xiao-Ming, Hu Xiao-Ying, Zeng Yi and Zheng Wei-Tao

**087301 Phase transformation in Mg–Sb<sub>3</sub>Te thin films**

Li Jun-Jian, Wang Guo-Xiang, Chen Yi-Min, Shen Xiang, Nie Qiu-Hua, Lü Ye-Gang, Dai Shi-Xun and Xu Tie-Feng

(Continued on the Bookbinding Inside Back Cover)

- 087501 Exchange interaction between vortex and antivortex**  
Liu Yan, Li Hua-Nan, Hu Yong and Du An
- 087502 Magnetic field control of ferroelectric polarization and magnetization of  $\text{LiCu}_2\text{O}_2$  compound**  
Qi Yan and Du An
- 087503 Large coercivity and unconventional exchange coupling in manganese-oxide-coated manganese–gallium nanoparticles**  
Feng Jun-Ning, Liu Wei, Geng Dian-Yu, Ma Song, Yu Tao, Zhao Xiao-Tian, Dai Zhi-Ming, Zhao Xin-Guo and Zhang Zhi-Dong
- 087504 Influence of magnetic layer thickness on  $[\text{Fe}_{80}\text{Ni}_{20}\text{-O/SiO}_2]_n$  multilayer thin films**  
Wei Jian-Qing, Geng Hao, Xu Lei, Wang Lai-Sen, Chen Yuan-Zhi, Yue Guang-Hui and Peng Dong-Liang
- 087701 Rational doping for zinc oxide and its influences on morphology and optical properties**  
Xia Yu-Jing, Guan Zi-Sheng and He Tao
- 087802 Thickness dependence of the optical constants of oxidized copper thin films based on ellipsometry and transmittance**  
Gong Jun-Bo, Dong Wei-Le, Dai Ru-Cheng, Wang Zhong-Ping, Zhang Zeng-Ming and Ding Ze-Jun
- 087803 Raman scattering in  $\text{In/InO}_x$  core–shell structured nanoparticles**  
Wang Meng, Tian Ye, Zhang Jian-Ming, Guo Chuan-Fei, Zhang Xin-Zheng and Liu Qian
- 087804 Thermal effect of  $\text{Ge}_2\text{Sb}_2\text{Te}_5$  in phase change memory device**  
Li Jun-Tao, Liu Bo, Song Zhi-Tang, Ren Kun, Zhu Min, Xu Jia, Ren Jia-Dong, Feng Gao-Ming, Ren Wan-Chun and Tong Hao
- 087805 The engineering of doxorubicin-loaded liposome-quantum dot hybrids for cancer theranostics**  
Bowen Tian, Wafa' T. Al-Jamal and Kostas Kostarelos
- 087806 A tunable infrared plasmonic polarization filter with asymmetrical cross resonator**  
Chen Xi-Yao, Zhong Yuan-Gang, Jiang Jun-Zhen, Zeng Xia-Hui, Fu Ping, Qiu Yi-Shen and Li Hui
- 087807 Synthesis of Au nanorods in a low pH solution via seed-media method**  
Ma Xiao, Feng Jin-Yang, You Fang-Fang, Ma Juan, Zhao Xiu-Jian and Wang Moo-Chin
- 088103 Growth of threaded AlN whiskers by a physical vapor transport method**  
Wang Jun, Zhao Meng, Zuo Si-Bin and Wang Wen-Jun
- 088104 Complete coverage of reduced graphene oxide on silicon dioxide substrates**  
Huang Jingfeng, Melanie Larisika, Chen Hu, Steve Faulkner, Myra A. Nimmo, Christoph Nowak and Alfred Tok Ing Yoong
- 088105 Templated synthesis of highly ordered mesoporous cobalt ferrite and its microwave absorption properties**  
Li Guo-Min, Wang Lian-Cheng and Xu Yao
- 088106 Properties of passive nano films on zircaloy-4 affected by defects induced by hydrogen permeation**  
Gu Jun-Ji, Ling Yun-Han, Zhang Rui-Qian, Dai Xun and Bai Xin-De
- 088107 Quantum transport characteristics in single and multiple N-channel junctionless nanowire transistors at low temperatures**  
Wang Hao, Han Wei-Hua, Ma Liu-Hong, Li Xiao-Ming and Yang Fu-Hua

*(Continued on the Bookbinding Inside Back Cover)*



**088201 Nonlinear dynamic characteristics and optimal control of a giant magnetostrictive film-shaped memory alloy composite plate subjected to in-plane stochastic excitation**

Zhu Zhi-Wen, Zhang Qing-Xin and Xu Jia

**088501 Comparison between N<sub>2</sub> and O<sub>2</sub> anneals on the integrity of an Al<sub>2</sub>O<sub>3</sub>/Si<sub>3</sub>N<sub>4</sub>/SiO<sub>2</sub>/Si memory gate stack**

Chu Yu-Qiong, Zhang Man-Hong, Huo Zong-Liang and Liu Ming

**088502 Chemical mechanical planarization of Ge<sub>2</sub>Sb<sub>2</sub>Te<sub>5</sub> using IC1010 and Politex reg pads in acidic slurry**

He Ao-Dong, Liu Bo, Song Zhi-Tang, Wang Liang-Yong, Liu Wei-Li, Feng Gao-Ming and Feng Song-Lin

**088802 High microwave absorption performances for single-walled carbon nanotube–epoxy composites with ultra-low loadings**

Liang Jia-Jie, Huang Yi, Zhang Fan, Li Ning, Ma Yan-Feng, Li Fei-Fei and Chen Yong-Sheng

**088803 Photoinduced degradation of organic solar cells with different microstructures**

Lu Chun-Xi, Yan Peng, Wang Jin-Ze, Song De and Jiang Chao

#### **RAPID COMMUNICATION**

**086103 Two-coupled structural modulations in charge-density-wave state of SrPt<sub>2</sub>As<sub>2</sub> superconductor**

Wang Li, Wang Zhen, Shi Hong-Long, Chen Zhen, Chiang Fu-Kuo, Tian Huan-Fang, Yang Huai-Xin, Fang Ai-Fang, Wang Nan-Lin and Li Jian-Qi

**086501 Influence of defects in SiC (0001) on epitaxial graphene**

Guo Yu, Guo Li-Wei, Lu Wei, Huang Jiao, Jia Yu-Ping, Sun Wei, Li Zhi-Lin and Wang Yi-Fei

#### **GENERAL**

**080201 Complex dynamical behaviors of compact solitary waves in the perturbed mKdV equation**

Yin Jiu-Li, Xing Qian-Qian and Tian Li-Xin

**080202 Model-based predictive controller design for a class of nonlinear networked systems with communication delays and data loss**

An Bao-Ran and Liu Guo-Ping

**080203 Improved locality-sensitive hashing method for the approximate nearest neighbor problem**

Lu Ying-Hua, Ma Ting-Huai, Zhong Shui-Ming, Cao Jie, Wang Xin and Abdullah Al-Dhelaan

**080204 Multi-symplectic method for the coupled Schrödinger–KdV equations**

Zhang Hong, Song Song-He, Zhou Wei-En and Chen Xu-Dong

**080205 Discrete event model-based simulation for train movement on a single-line railway**

Xu Xiao-Ming, Li Ke-Ping and Yang Li-Xing

**080206 A feedback control method for the stabilization of a nonlinear diffusion system on a graph**

Yu Xin, Xu Chao and Lin Qun

**080301 New operator-ordering identities and associative integration formulas of two-variable Hermite polynomials for constructing non-Gaussian states**

Fan Hong-Yi and Wang Zhen

**080302 A sufficient and necessary criterion for separability of bipartite quantum states**

Zhao Hui and Yu Xin-Yu

**080303 Security of a practical semi-device-independent quantum key distribution protocol against collective attacks**

Wang Yang, Bao Wan-Su, Li Hong-Wei, Zhou Chun and Li Yuan

**080304 An autobias control system for the electro-optic modulator used in a quantum key distribution system**

Chen Wen-Fen, Wei Zheng-Jun, Guo Li, Hou Li-Yan, Wang Geng, Wang Jin-Dong, Zhang Zhi-Ming, Guo Jian-Ping and Liu Song-Hao

**080305 Entanglement concentration for W-type entangled coherent states**

Sheng Yu-Bo, Liu Jiong, Zhao Sheng-Yang, Wang Lei and Zhou Lan

**080501 Control of fractional chaotic and hyperchaotic systems based on a fractional order controller**

Li Tian-Zeng, Wang Yu and Luo Mao-Kang

**080502 Solid-state resonant tunneling thermoelectric refrigeration in the cylindrical double-barrier nanostructure**

Liu Nian, Luo Xiao-Guang and Zhang Mao-Lian

**080503 Stochastic resonance in an over-damped linear oscillator**

Lin Li-Feng, Tian Yan and Ma Hong

**080504 Double coherence resonance of the FitzHugh–Nagumo neuron driven by harmonic velocity noise**

Song Yan-Li

**080505 Evacuation of pedestrians from a hall by game strategy update**

Wang Hao-Nan, Chen Dong, Pan Wei, Xue Yu and He Hong-Di

#### **ATOMIC AND MOLECULAR PHYSICS**

**083101 Influence of chirality on the thermal conductivity of single-walled carbon nanotubes**

Feng Ya, Zhu Jie and Tang Da-Wei

**083201 Semi-classical explanation for the dissociation control of  $H_2^+$**

Jia Zheng-Mao, Zeng Zhi-Nan, Li Ru-Xin and Xu Zhi-Zhan

**083302 A simple encapsulation method for organic optoelectronic devices**

Sun Qian-Qian, An Qiao-Shi and Zhang Fu-Jun

**083701 Production of CH ( $A^2\Delta$ ) by multi-photon dissociation of  $(CH_3)_2CO$ ,  $CH_3NO_2$ ,  $CH_2Br_2$ , and  $CHBr_3$  at 213 nm**

Li Sheng-Qiang, Xu Liang, Chen Yang-Qin, Deng Lian-Zhong and Yin Jian-Ping

#### **ELECTROMAGNETISM, OPTICS, ACOUSTICS, HEAT TRANSFER, CLASSICAL MECHANICS, AND FLUID DYNAMICS**

**084202 Relation between Airy beams and triple-cusp beams**

Ren Zhi-Jun, Li Xiao-Dong, Jin Hong-Zhen, Chen Chen and Wu Jiang-Miao

**084203 Electronic and optical properties of  $TiO_2$  and its polymorphs by Z-scan method**

S. Divya, V P N Nampoory, P Radhakrishnan and A Mujeeb

**084204 Large phase shift of spatial soliton in lead glass by cross-phase modulation in pump-signal geometry**

Shou Qian, Liu Dong-Wen, Zhang Xiang, Hu Wei and Guo Qi

**084205 A new kind of superimposing morphology for enhancing the light scattering in thin film silicon solar cells: Combining random and periodic structure**

Huang Zhen-Hua, Zhang Jian-Jun, Ni Jian, Wang Hao and Zhao Ying

**084206 Multipole resonance in the interaction of a spherical Ag nanoparticle with an emitting dipole**

Liu Jia-Dong, Song Feng, Zhang Jun, Liu Shu-Jing, Wang Feng-Xiao and Wang Li-Chao

**084207 Heralded linear optical quantum Fredkin gate based on one auxiliary qubit and one single photon detector**

Zhu Chang-Hua, Cao Xin, Quan Dong-Xiao and Pei Chang-Xing

**084208 Experimental study on the Stokes effect in disordered birefringent microstructure fibers**

Zhao Yuan-Yuan, Zhou Gui-Yao, Li Jian-She, Zhang Zhi-Yuan and Han Ying

**084501 Broadband energy harvesting via magnetic coupling between two movable magnets**

Fan Kang-Qi, Xu Chun-Hui, Wang Wei-Dong and Fang Yang

**084701 Heat transfer analysis in the flow of Walters' B fluid with a convective boundary condition**

T. Hayat, Sadia Asad, M. Mustafa and Hamed H. Alsulami

**084702 Simulation of fluid-structure interaction in a microchannel using the lattice Boltzmann method and size-dependent beam element on a graphics processing unit**

Vahid Esfahanian, Esmaeil Dehdashti and Amir Mehdi Dehrouye-Semnani

#### **PHYSICS OF GASES, PLASMAS, AND ELECTRIC DISCHARGES**

**085201 Compound sawtooth in EAST LHCD plasma: An experimental study**

Xu Li-Qing, Hu Li-Qun, Chen Kai-Yun and Li Miao-Hui

**085202 Simulation of nanoparticle coagulation in radio-frequency capacitively coupled C<sub>2</sub>H<sub>2</sub> discharges**

Liu Xiang-Mei, Li Qi-Nan and Xu Xiang

**085203 Shadowgraph investigation of plasma shock wave evolution from Al target under 355-nm laser ablation**

Liu Tian-Hang, Hao Zuo-Qiang, Gao Xun, Liu Ze-Hao and Lin Jing-Quan

#### **CONDENSED MATTER: STRUCTURAL, MECHANICAL, AND THERMAL PROPERTIES**

**086104 Simulation of temporal characteristics of ion-velocity susceptibility to single event upset effect**

Geng Chao, Xi Kai, Liu Tian-Qi, Gu Song and Liu Jie

**086301 Study on lattice vibrational properties and Raman spectra of Bi<sub>2</sub>Te<sub>3</sub> based on density-functional perturbation theory**

Feng Song-Ke, Li Shuang-Ming and Fu Heng-Zhi

**086401 Decline of nucleation in the heating process with a high heating rate**

Yang Gao-Lin, Lin Xin, Song Meng-Hua, Hu Qiao, Wang Zhi-Tai and Huang Wei-Dong

#### **CONDENSED MATTER: ELECTRONIC STRUCTURE, ELECTRICAL, MAGNETIC, AND OPTICAL PROPERTIES**

**087101 Electronic structures and optical properties of III<sub>A</sub>-doped wurtzite Mg<sub>0.25</sub>Zn<sub>0.75</sub>O**

Zheng Shu-Wen, He Miao, Li Shu-Ti and Zhang Yong

- 087102 Theory of phonon-modulated electron spin relaxation time based on the projection–reduction method**  
Nam Lyong Kang and Sang Don Choi
- 087103 Investigations of the half-metallic behavior and the magnetic and thermodynamic properties of half-Heusler CoMnTe and RuMnTe compounds: a first-principles study**  
T. Djaafri, A. Djaafri, A. Elias, G. Murtaza, R. Khenata, R. Ahmed, S. Bin Omran and D. Rached
- 087201 An improved EEHEMT model for kink effect on AlGaIn/GaN HEMT**  
Cao Meng-Yi, Lu Yang, Wei Jia-Xing, Chen Yong-He, Li Wei-Jun, Zheng Jia-Xin, Ma Xiao-Hua and Hao Yue
- 087202 Valley selection rule in a Y-shaped zigzag graphene nanoribbon junction**  
Zhang Lin and Wang Jun
- 087203 Synthesis and electrical conductivity of nanocrystalline tetragonal FeS**  
Zeng Shu-Lin, Wang Hui-Xian and Dong Cheng
- 087302 Stability and electronic structure studies of LaAlO<sub>3</sub>/SrTiO<sub>3</sub> (110) heterostructures**  
Du Yan-Ling, Wang Chun-Lei, Li Ji-Chao, Xu Pan-Pan, Zhang Xin-Hua, Liu Jian, Su Wen-Bin and Mei Liang-Mo
- 087303 Fano-like resonance characteristics of asymmetric Fe<sub>2</sub>O<sub>3</sub>@Au core/shell nanorice dimer**  
Wang Bin-Bing, Zhou Jun, Zhang Hao-Peng and Chen Jin-Ping
- 087304 Bipolar resistance switching in the fully transparent BaSnO<sub>3</sub>-based memory device**  
Zhang Ting, Yin Jiang, Zhao Gao-Feng, Zhang Wei-Feng, Xia Yi-Dong and Liu Zhi-Guo
- 087305 A two-dimensional fully analytical model with polarization effect for off-state channel potential and electric field distributions of GaN-based field-plated high electron mobility transistor**  
Mao Wei, She Wei-Bo, Yang Cui, Zhang Chao, Zhang Jin-Cheng, Ma Xiao-Hua, Zhang Jin-Feng, Liu Hong-Xia, Yang Lin-An, Zhang Kai, Zhao Sheng-Lei, Chen Yong-He, Zheng Xue-Feng and Hao Yue
- 087306 Spin-excited states and rectification in an organic spin rectifier**  
Zuo Meng-Ying, Hu Gui-Chao, Li Ying, Ren Jun-Feng and Wang Chuan-Kui
- 087307 Forward and reverse electron transport properties across a CdS/Si multi-interface nanoheterojunction**  
Li Yong, Wang Ling-Li, Wang Xiao-Bo, Yan Ling-Ling, Su Li-Xia, Tian Yong-Tao and Li Xin-Jian
- 087308 Topological quantum-phase coherence in full counting statistics of transport electrons with two-body interaction**  
Guo Xiao-Fang, Xue Hai-Bin and Liang Jiu-Qing
- 087401 In-plane optical spectral weight redistribution in the optimally doped Ba<sub>0.6</sub>K<sub>0.4</sub>Fe<sub>2</sub>As<sub>2</sub> superconductor**  
Xu Bing, Dai Yao-Min, Xiao Hong, R. P. S. M. Lobo and Qiu Xiang-Gang
- 087402 Fabrication and properties of the meander nanowires based on ultra-thin Nb films**  
Zhao Lu, Jin Yi-Rong, Li Jie, Deng Hui and Zheng Dong-Ning
- 087505 The spin dynamics of the random transverse Ising chain with a double-Gaussian disorder**  
Liu Zhong-Qiang, Jiang Su-Rong and Kong Xiang-Mu
- 087506 Magnetic interaction in the metamaterial/magnet system**  
M. K. Alqadi and F. Y. Alzoubi

- 087702 Effect of structural parameters of Gaussian repaired pit on light intensity distribution inside  $\text{KH}_2\text{PO}_4$  crystal**  
Xiao Yong, Chen Ming-Jun, Cheng Jian, Liao Wei, Wang Hai-Jun and Li Ming-Quan
- 087808 Microwave-promoted pure host phase for red emission  $\text{CaS:Eu}^{2+}$  phosphor from single  $\text{CaSO}_4$  precursor and the photoluminescence property**  
Ma Jian, Lu Qi-Fei, Wang Yan-Ze, Lu Zhi-Juan, Sun Liang, Dong Xiao-Fei and Wang Da-Jian
- 087809 Concentration effect of the near-infrared quantum cutting of 1788-nm luminescence of  $\text{Tm}^{3+}$  ion in  $(\text{Y}_{1-x}\text{Tm}_x)_3\text{Al}_5\text{O}_{12}$  powder phosphor**  
Chen Xiao-Bo, Li Song, Ding Xian-Lin, Yang Xiao-Dong, Liu Quan-Lin, Gao Yan, Sun Ping and Yang Guo-Jian
- 087810 Effect of high-temperature annealing on AlN thin film grown by metalorganic chemical vapor deposition**  
Wang Wei-Ying, Jin Peng, Liu Gui-Peng, Li Wei, Liu Bin, Liu Xing-Fang and Wang Zhan-Guo
- 087811 Effect of NaCl doped into Bphen layer on the performance of tandem organic light-emitting diodes**  
Xiao Zhi-Hui, Wu Xiao-Ming, Hua Yu-Lin, Bi Wen-Tao, Wang Li, Zhang Xin, Xin Li-Wen and Yin Shou-Gen
- INTERDISCIPLINARY PHYSICS AND RELATED AREAS OF SCIENCE AND TECHNOLOGY**
- 088108 Effects of graphene defects on Co cluster nucleation and intercalation**  
Xu Wen-Yan, Huang Li, Que Yan-De, Lin Xiao, Wang Ye-Liang, Du Shi-Xuan and Gao Hong-Jun
- 088109 Phase field crystal study of the crystallization modes within the two-phase region**  
Yang Tao, Zhang Jing, Long Jian, Long Qing-Hua and Chen Zheng
- 088110 Nucleation of GaSb on GaAs (001) by low pressure metal-organic chemical vapor deposition**  
Wang Lian-Kai, Liu Ren-Jun, Yang Hao-Yu, Lü You, Li Guo-Xing, Zhang Yuan-Tao and Zhang Bao-Lin
- 088111 Annealing effect of platinum-incorporated nanowires created by focused ion/electron-beam-induced deposition**  
Fang Jing-Yue, Qin Shi-Qiao, Zhang Xue-Ao, Liu Dong-Qing and Chang Sheng-Li
- 088112 Epitaxial growth of  $\text{Ge}_{1-x}\text{Sn}_x$  films with  $x$  up to 0.14 grown on Ge (001) at low temperature**  
Tao Ping, Huang Lei, Cheng H H, Wang Huan-Hua and Wu Xiao-Shan
- 088113 Modeling for V-O<sub>2</sub> reactive sputtering process using a pulsed power supply**  
Wang Tao, Yu He, Dong Xiang, Jiang Ya-Dong, Chen Chao and Wu Ro-Land
- 088114 Large-scale photonic crystals with inserted defects and their optical properties**  
Li Chao-Rong, Li Juan, Yang Hu, Zhao Yong-Qiang, Wu Yan, Dong Wen-Jun and Chen Ben-Yong
- 088401 Complete eigenmode analysis of a ladder-type multiple-gap resonant cavity**  
Zhang Chang-Qing, Ruan Cun-Jun, Zhao Ding, Wang Shu-Zhong and Yang Xiu-Dong
- 088402 Analysis of the injection-locked magnetron with a mismatched circulator**  
Yue Song, Zhang Zhao-Chuan and Gao Dong-Ping
- 088503 A SQUID gradiometer module with large junction shunt resistors**  
Qiu Yang, Liu Chao, Zhang Shu-Lin, Zhang Guo-Feng, Wang Yong-Liang, Li Hua, Zeng Jia, Kong Xiang-Yan and Xie Xiao-Ming

*(Continued on the Bookbinding Inside Back Cover)*

- 088504 A novel high performance TFS SJ IGBT with a buried oxide layer**  
Zhang Jin-Ping, Li Ze-Hong, Zhang Bo and Li Zhao-Ji
- 088505 Estimation of pulsed laser-induced single event transient in a partially depleted silicon-on-insulator 0.18- $\mu\text{m}$  MOSFET**  
Bi Jin-Shun, Zeng Chuan-Bin, Gao Lin-Chun, Liu Gang, Luo Jia-Jun and Han Zheng-Sheng
- 088701 Realization of a broadband terahertz wavelength-selective coupling based on five-core fibers**  
Li Xu-You, Yu Ying-Ying, Sun Bo and He Kun-Peng
- 088702 A study of multi-trapping of tapered-tip single fiber optical tweezers**  
Liang Pei-Bo, Lei Jiao-Jie, Liu Zhi-Hai, Zhang Yu and Yuan Li-Bo
- 088703 Colloidal monolayer self-assembly and its simulation via cellular automaton model**  
Wu Yi-Zhi, Chen Chen, Xu Xiao-Liang, Liu Yun-Xi, Shao Wei-Jia, Yin Nai-Qiang, Zhang Wen-Ting, Ke Jia-Xin and Fang Xiao-Tian
- 088901 Modeling walking behavior of pedestrian groups with floor field cellular automaton approach**  
Lu Li-Li, Ren Gang, Wang Wei and Wang Yi
- 088902 An effective method to improve the robustness of small-world networks under attack**  
Zhang Zheng-Zhen, Xu Wen-Jun, Zeng Shang-You and Lin Jia-Ru
- GEOPHYSICS, ASTRONOMY, AND ASTROPHYSICS**
- 089201 An approach to estimating and extrapolating model error based on inverse problem methods: Towards accurate numerical weather prediction**  
Hu Shu-Juan, Qiu Chun-Yu, Zhang Li-Yun, Huang Qi-Can, Yu Hai-Peng and Chou Ji-Fan
- 089401 Test particle simulations of resonant interactions between energetic electrons and discrete, multi-frequency artificial whistler waves in the plasmasphere**  
Chang Shan-Shan, Ni Bin-Bin, Zhao Zheng-Yu, Gu Xu-Dong and Zhou Chen
- 089501 The mass limit of white dwarfs with strong magnetic fields in general relativity**  
Wen De-Hua, Liu He-Lei and Zhang Xiang-Dong

JUST FOR AUTHORS  
— CHINESE PHYSICS B